Contributions of Active Site Residues to the Partial and Overall Catalytic Activities of Human *S*-Adenosylhomocysteine Hydrolase†

Philip Elrod,‡,§ Jinsong Zhang,‡ Xiaoda Yang,|| Dan Yin,⊥ Yongbo Hu, Ronald T. Borchardt, and Richard L. Schowen*

Departments of Molecular Biosciences and Pharmaceutical Chemistry, Simons Research Laboratories, The University of Kansas, Lawrence, Kansas 66047

Received March 4, 2002; Revised Manuscript Received April 24, 2002

ABSTRACT: Residues glutamate 156 (E156), aspartate 190 (D190), asparagine 181 (N181), lysine 186 (K186), and asparagine 191 (N191) in the active site of *S*-adenosylhomocysteine (AdoHcy) hydrolase have been mutated to alanine (A). AdoHcy hydrolase achieves catalysis of AdoHcy hydrolysis to adenosine (Ado) and homocysteine (Hcy) by means of a redox partial reaction (3′-oxidation of AdoHcy at the beginning and 3′-reduction of Ado at the end of the catalytic cycle) spanning an elimination/addition partial reaction (elimination of Hcy from the oxidized substrate and addition of water to generate the oxidized product), with the enzyme in an open NAD^+ form in the ligand-free state and in a closed NADH form during the elimination/addition partial reaction. Mutation K186A reduces the rate of a model enzymatic reaction for the redox partial reaction by a factor of 280000 and the rate of a model reaction for the elimination/addition partial reaction by a factor of 24000, consistent with a primary catalytic role in both partial reactions as a proton donor/acceptor at the 3′-OH/3′-keto center. Secondary roles for N181 and N191 in localizing the flexible side chain of K186 in a catalytically effective position are supported by rate reduction factors for N181A of 2500 (redox) and 240 (elimination/addition) and for N191A of 730 (redox) and 340 (elimination/addition). A role of D190 in orienting the substrate for effective transition-state stabilization is consistent with rate reduction factors of 1300 (redox) and 30 (elimination/addition) for D190A. Residue E156 may act to maintain K186 in the desired protonation state: rate deduction factors are 1100 (redox) and 70 (elimination/addition). The mutational increases in free energy barriers for k_{cat}/K_M are described by a linear combination of the effects for the partial reactions with the coefficients equal to the fractional degree that each partial reaction determines the rate for k_{cat}/K_M. A similar linear equation for k_{cat} overestimates the barrier increase by a uniform 5 kJ/mol, probably reflecting reactant-state stabilization by the wild-type enzyme that is abolished by the mutations.

S-Adenosylhomocysteine (AdoHcy)[1] hydrolase (EC 3.3.1.1) catalyzes the reversible interconversion of *S*-adenosylhomocysteine (AdoHcy) with adenosine (Ado) and homocysteine (Hcy) (*1*, *2*). The enzyme is of considerable interest for questions of the coupling between catalytic function and protein motion, since its large domain−domain oscillation in the free state is completely arrested during the catalytic cycle (the domain structure of the monomeric subunit of the homotetrameric enzyme is shown in Figure 1). In addition, AdoHcy hydrolase is considered a drug target for the therapy of viral (*3*, *4*) and parasitic infections (*5*), as well as cardiovascular conditions (*6*).

AdoHcy hydrolase catalyzes the hydrolytic fission of the C−S bond of AdoHcy by means of a complex strategy (Figure 2). The human enzyme has a tightly bound NAD^+ cofactor in each of the four identical active sites in its homotetrameric structure (cf. Figure 1). Upon binding of AdoHcy and closing of the active site, the substrate is oxidized by the cofactor to the 3′-keto stage. The 3′-keto group serves to activate the 4′-CH bond, allowing elimination of the Hcy anion with formation of a 4′−5′ olefinic linkage conjugated to the 3′-keto group. Now Michael addition of water produces 3′-ketoadenosine (3′-ketoAdo), and in the final stage of catalysis, the NADH cofactor reduces the intermediate to the product Ado (*1*). Thus, the catalytic cycle consists of two partial reactions: an elimination/addition partial reaction in which Hcy is eliminated and water is added and a redox partial reaction which spans the elimination/

† This work was supported by a grant from the National Institutes of Health (GM-29332).

* To whom correspondence should be addressed. Telephone: 785-864-4080. Fax: 785-864-5736. E-mail: rschowen@ku.edu.

‡ Contributed equally to the current study.

§ Current address: Pharmacia Corp., 7000 Portage Road 1400-89-1, Kalamazoo, MI 49001.

|| Current address: Department of Chemical Biology, School of Pharmaceutical Science, Peking University Health Science Center, Beijing, China 100083.

⊥ Current address: Department of Vaccine Pharmaceutical Research, Merck Research Laboratories, West Point, PA 19486.

[1] Abbreviations: Ado, adenosine; AdoHcy hydrolase, *S*-adenosylhomocysteine hydrolase; CD, circular dichroism; AdoHcy, *S*-adenosylhomocysteine; Hcy, homocysteine; EDDFHA, (*E*)-5′,6′-didehydro-6′-deoxy-6′-fluorohomoadenosine; DFHHA, 6′-deoxy-6′-fluoro-5′-hydroxyhomoadenosine; EDTA, ethylenediaminetetraacetic acid; FPLC, fast protein liquid chromatography; IPTG, isopropyl β-D-thiogalactopyranoside; 3′-ketoAdo, 3′-ketoadenosine; NAD^+, nicotinamide adenine dinucleotide (oxidized); NADH, nicotinamide adenine dinucleotide (reduced); PCR, polymerase chain reaction; SDS−PAGE, sodium dodecyl sulfate−polyacrylamide gel electrophoresis; NepA, neplanocin A; 2 × YT, 2 × yeast tryptone.

10.1021/bi025771p CCC: $22.00
Published on Web 06/01/2002

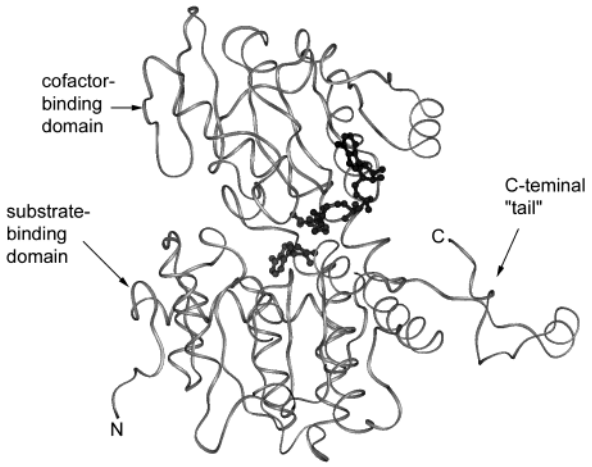

FIGURE 1: The domain structure of human AdoHcy hydrolase (*9*), shown for a monomeric subunit of the homotetrameric enzyme. The closed form of the enzyme, characteristic of the complex with 3′-keto substrate bound and cofactor in the NADH oxidation state, is shown. In the absence of substrate, with the cofactor in the NAD^+ oxidation state, the enzyme is in the open form with the two domains oscillating against each other through an angle of about 17° (*21*).

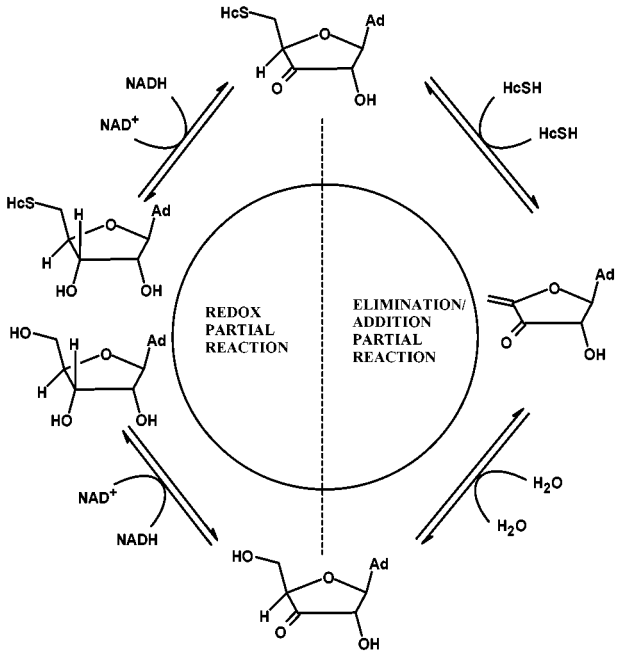

FIGURE 2: The catalytic cycle of AdoHcy hydrolase (*1*), consisting of an elimination/addition partial reaction, which is spanned by a redox partial reaction. In the substrate-free form, the E·NAD^+ enzyme is open with its two domains in motion (*21*). Binding of substrate induces a cessation of the motion, followed by oxidation of substrate at the 3′-position. The keto form of the substrate, activated for elimination of the 4′-proton and the 5′-substituent (Hcy in the hydrolytic direction, water in the synthetic direction), undergoes elimination. Michael addition of the complementary 5′-substituent (water in the hydrolytic direction, Hcy in the synthetic direction) and a 4′-proton produces the 3′-keto product. In the second event of the redox partial reaction, product is generated by a 3′-reduction reaction. The enzyme remains in the closed form throughout the elimination/addition sequence.

addition partial reaction, generating a reactive keto substrate at the beginning of the cycle and reducing the keto product at the end of the cycle.

The availability of several crystal structures that are relevant to the catalytic function (*7*−*9*), particularly that of

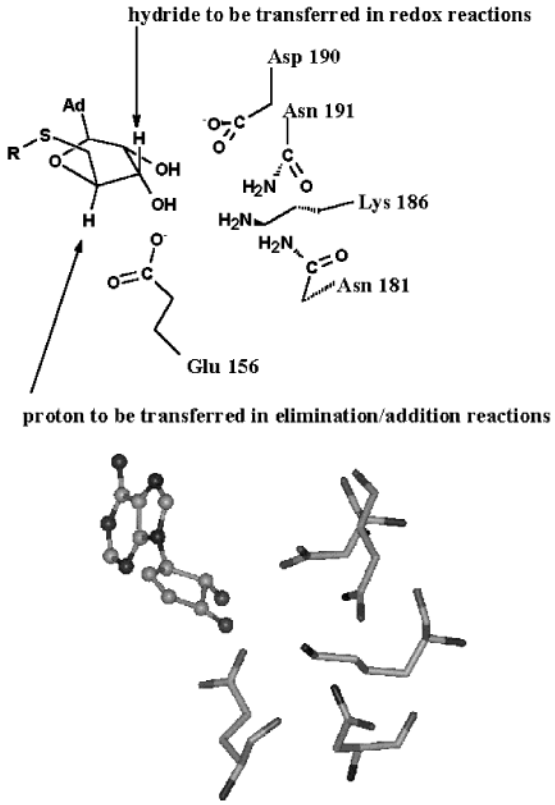

FIGURE 3: Residues chosen for mutation and characterization in the present study. The upper representation shows the schematic relationship of the five residues (D190, N191, K186, N181, and E156) to the bound substrate. The lower structure is taken from the structure of Turner et al. (*9*) and shows the three-dimensional relationship of the five residues to the location of the keto substrate analogue.

Turner et al. (*9*), which has captured the enzyme in the "closed" form within which its catalytic functions are expressed, allows the formulation of hypotheses about the residues that may affect the catalytic acceleration for this enzyme. In the present paper, we report an investigation centered on five residues that could reasonably be anticipated to produce some acceleration of either the redox or elimination/addition partial reactions. Figure 3 identifies these residues, and Figure 4 specifies some of the catalytic roles they may take. The caption of Figure 4 gives some relevant distances from the crystal structure (*9*), and both the caption and the body of Figure 4 give some detail on these hypotheses. We report here the mutation of each of the five residues to alanine, so as to remove their capacity for any of the suspected catalytic roles. Each of the mutant enzymes has been purified, reconstituted fully with cofactor, and characterized with respect to primary, secondary/tertiary, and quaternary structure.

The mutant enzymes have also been characterized functionally. The catalytic constants k_{cat}/K_M and k_{cat} for conversion of AdoHcy to Ado and Hcy have been obtained, and in addition, rate constants have been measured for two model reactions of the enzymes, one of which simulates some features of the redox partial reaction and another that simulates some features of the elimination/addition partial reaction. These model reactions are portrayed in Figures 5 and 6. Figure 5 compares the reaction of the enzyme with neplanocin A (NepA) with the redox partial reaction (*10*); the two reactions share some characteristics. Figure 6

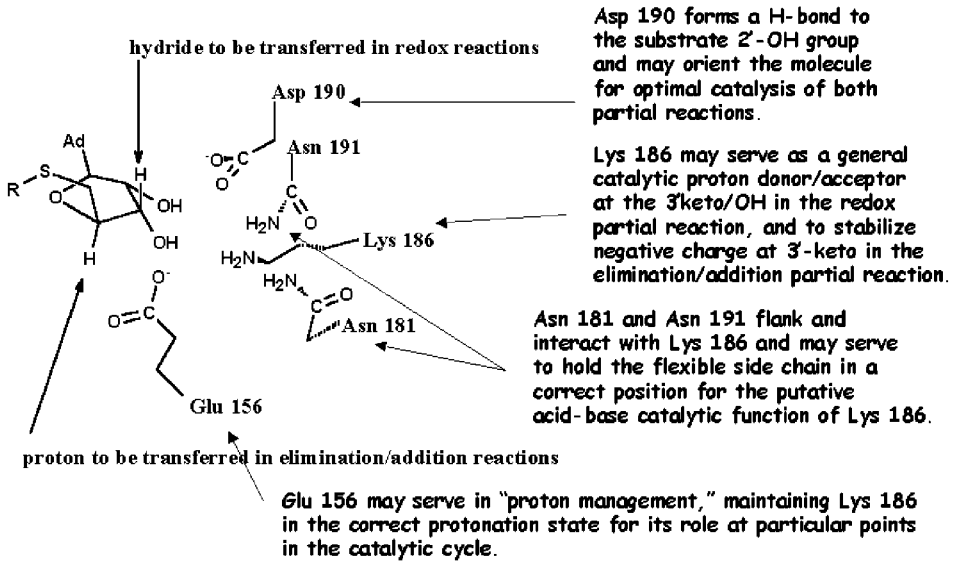

FIGURE 4: Roles in the catalytic acceleration of AdoHcy hydrolase hypothesized for residues D190, K186, N181/N191, and E156 for both the redox partial reaction and the elimination/addition partial reaction. D190 may play a general role in substrate orientation. K186 is suspected of accelerating hydride transfer from and to C-3′ by proton removal and donation (or equivalent hydrogen bonding) at the 3′-hydroxyl/keto group. In the elimination/addition reaction, negative charge is expected to appear in the transition state on the keto oxygen at the 3′-center, and K186 may donate a hydrogen bond to stabilize this charge. N181 and N191 may serve to localize the flexible side chain of K186 appropriately for its catalytic functions. Because the ϵ-amino group of K186 must be protonated when it functions as a proton donor and unprotonated when it functions as a proton acceptor, appropriately timed transport of protons to and from the amino group may be necessary. We call this function proton management and consider that E156 may assist in achieving it. Distances relevant to the potential catalytic roles are as follows: C2′-hydroxyl O to nearest carboxyl O of D190, 3.1 Å; ϵ-amino N of K186 to amido N of N191, 2.7 Å; ϵ-amino N of K186 to amido N of N181, 2.6 Å; ϵ-amino N of K186 to C3′-keto O, 3.1 Å; ϵ-amino N of K186 to nearest carboxyl O of E156, 4.2 Å.

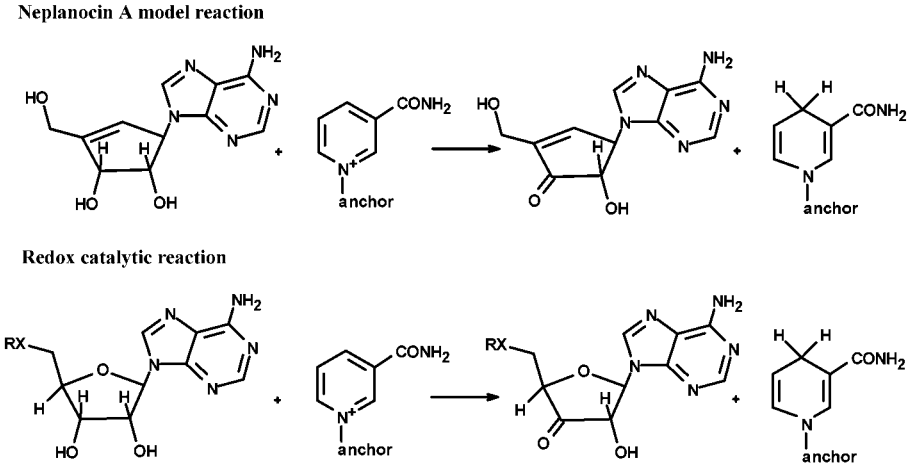

FIGURE 5: Comparison of the NepA model reaction with the redox partial reaction of the catalytic cycle. In both reactions, the 3′-OH functional group undergoes oxidation by the NAD^+ cofactor. The geometric features of the catalytic reaction in the immediate neighborhood of the 3′-center are well simulated in the model reaction, but the electronic features and more remote geometrical features are not. The model reaction is lacking the oxa center of the ribose, the forming 3′-keto group is conjugated, and the 4′-center is planar instead of tetrahedral, all features that contrast with those of the catalytic reaction. The term anchor refers to the adenylylphosphoribosyl moiety of the cofactor, which anchors it to the enzyme.

compares the reaction of the alternative substrate (*E*)-5′,6′-didehydro-6′-deoxy-6′-fluorohomoadenosine (EDDFHA) with the elimination/addition partial reaction (*11*); some characteristics of the two reactions are again shared. A unified interpretation of the data is presented below.

EXPERIMENTAL PROCEDURES

Materials. Competent JM109 *Escherichia coli* cells were obtained from Promega (Madison, WI). Bacterial strains, containing the recombinant plasmid pPROKcd20 (*12*) inserted with the open reading frame of human placental AdoHcy hydrolase (Clonetech, Palo Alto, CA), were provided to our laboratory by Dr. Michael Hershfield (Duke University, Durham, NC). Midrange protein molecular weight markers were obtained from Promega. Pfu DNA polymerase was purchased from Stratagene (La Jolla, CA). *Dpn*I was purchased from New England Biolabs (Beverly, MA). Primers for thermal cycling were obtained from Sigma-Genosys (The Woodlands, TX). Primers for sequencing were obtained from Li-Cor (Lincoln, NE). The miniprep plasmid purification kit was purchased from Qiagen (Valencia, CA). The sequencing kit was purchased from Amersham Corp. (Arlington Heights, IL). Purified nicotinamide adenine dinucleotide, oxidized (NAD^+) and reduced (NADH) forms,

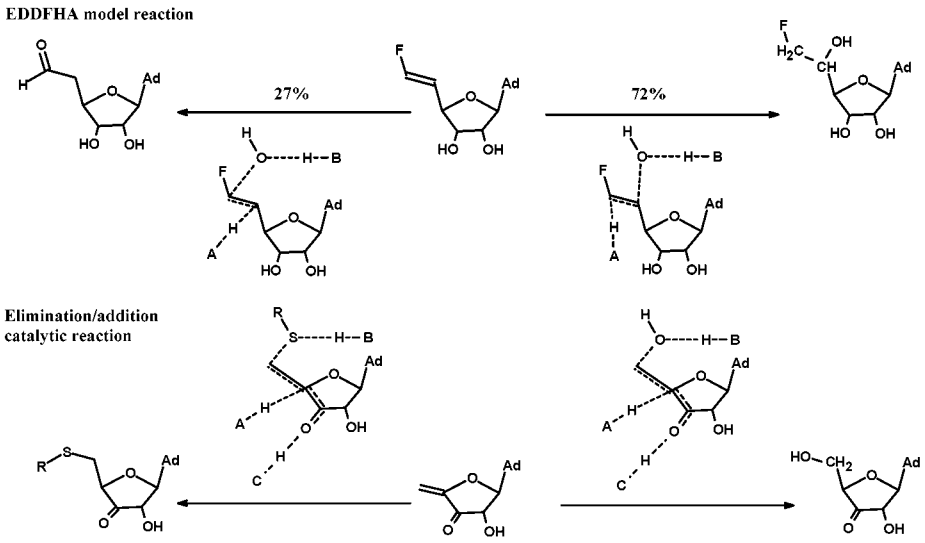

FIGURE 6: Comparison of the EDDFHA model reaction (top) with the elimination/addition partial reaction of the catalytic cycle (bottom). Schematic structures illustrating probable important transition-state interactions are shown over the arrows. The resemblance of the reactant-state molecules between the two reactions is not close. The chemical interactions around the olefinic linkage are to some extent reproduced in the model reaction, although the locus of the interactions is shifted further from the ribose ring in the model reactions. Interactions at the 3′-keto center are absent from the model reaction in which the 3′-OH functional group has not been oxidized.

and ampicillin were purchased from Sigma Chemical Co. (St. Louis, MO). G-25 M Sephadex size-exclusion columns were purchased from Amersham Pharmacia Biotech (Arlington Heights, IL). DEAE-cellulose, Sephacryl S-300, and Q-Sepharose were purchased from Pharmacia (Piscataway, NJ). Isopropyl β-D-thiogalactopyranoside (IPTG) was obtained from Fisher Biotech (Pittsburgh, PA). Pure EDDFHA, for use in mutant enzyme characterizations, was provided by Dr. Morris Robins (Department of Chemistry, Brigham Young University, Provo, UT). Ado, Hcy, AdoHcy, calf intestine Ado deaminase, egg white lysozyme, and bovine serum albumin were purchased from Sigma. 5,5′-dithiobis-(2-nitrobenzic acid) (DTNB) was purchased from Fluka Chemicals (Ronkonkoma, NY).

Preparation of Mutants of AdoHcy Hydrolase. Primers were designed using the program Oligo Primer from Oligo Etc. (Bethel, ME). The primers were designed to introduce a single- or double-base mutation that would change the codon for a chosen single amino acid residue to a codon for alanine. Each primer was designed to fit the following requirements: (i) each primer must be 20−30 base pairs in length; (ii) each primer must contain a well-balanced proportion of each of the base pairs A-T and C-G; (iii) each primer should contain the mutation in the middle of its sequence; and (iv) there should be no sequence repeats of five base pairs at any point or of three base pairs at the ends. Primers were created for the forward and reverse of each sequence corresponding to the double-stranded plasmid DNA. These computer-designed primers were synthesized and purified using reversed-phase HPLC by Sigma-Genosys.

Site-directed mutations were created using the QuikChange mutagenesis kit (Stratagene). After completion of the thermal cycles, the parental template DNA was destroyed by the addition of 2 units of *Dpn*I to the reaction and incubation for 1 h at 37 °C. The product was verified by agarose gel electrophoresis. The amplified product was then transformed into JM109 competent cells. Small-scale purification of plasmid made use of the "miniprep" kit from QIAGEN according to the manual provided. DNA was quantified spectrophotometrically or electrophoretically. The purified plasmid was then sequenced to verify the mutations. The Sanger method was used for sequencing the purified plasmid DNA. Sequence comparisons against the original sequence of the AdoHcy hydrolase gene were made to verify that all mutations were single-residue mutations. Verified mutants were then recovered from permanent storage and used for large-scale harvest of protein.

Permanent cultures of JM109 bacterial cells containing verified mutant genes were available as 100 μL aliquots frozen at −80 °C. For each mutant, 100 μL of permanent culture was used to inoculate 10 mL of 2 × YT broth. The inoculated broth was grown overnight at 37 °C in a LABLINE Orbit Environ shaker, shaken continuously at 200 rpm. Overnight culture (100 μL) was used to inoculate 250 mL of 2 × YT medium containing 75 μM ampicillin in a 1 Lr flask, with a total of four flasks used. The cells were incubated at 37 °C until the absorbance at 600 nm reached 0.2. Then IPTG was added to achieve a final concentration of 1 mM, and the culture was incubated for an additional 14 h.

Purification of Mutants of AdoHcy Hydrolase. Recombinant human placental wild-type or mutant AdoHcy hydrolase was purified by a modification of the procedure described by Yuan et al. (*13*). Cells from IPTG-induced cultures were harvested by centrifugation at 6000 rpm in a Beckman centrifuge with a JA-14 rotor. The cells were washed with 0.9% NaCl to remove the remainder of the 2 × YT medium. The cells were again centrifuged at 6000 rpm and washed again. The cell pellet was resuspended in 40 mL of 50 mM Tris-HCl buffer at pH 7.5, containing 2 mM EDTA. The solution was transferred to a 250 mL lyophilizing chamber. The cells were treated with egg white lysozyme (1 mg/mL) for 30 min at 0 °C, followed by a fast freeze-and-thaw procedure with a dry ice/ethanol bath and a 37 °C water bath three times until the cells had a jellylike consistency. The cell lysate was then transferred to 50 mL centrifuge tubes and centrifuged at 20000 rpm in a Beckman Model J2-21 using a JA-22 rotor. Nucleic acids were removed from the

cell-free extract (supernatant from the last step) by mixing with DEAE-cellulose, equilibrated with 0.1 M potassium phosphate, pH 7.2, containing 1 mM EDTA. Proteins were eluted three times with 100 mL of 0.1 M PBE buffer (0.1 M potassium phosphate, pH 7.2, containing 1 mM EDTA). Ammonium sulfate (70%) was added gradually to precipitate proteins overnight. The precipitate was collected by centrifugation at 10000 rpm for 20 min. The pellet was resuspended in 10 mM potassium phosphate, pH 7.2, containing 1 mM EDTA, and subjected to chromatography on a column (2.8 × 100 cm) of Sephacryl S-300. The column was equilibrated and eluted with 50 mM potassium phosphate, pH 7.2, containing 1 mM EDTA. Fractions containing AdoHcy hydrolase, as double checked by SDS−PAGE, were combined. The final purification was accomplished by Q-Sepharose chromatography (2.8 × 25 cm column). The column was equilibrated with 10 mM potassium phosphate, pH 7.2, containing 1 mM EDTA. The protein was eluted from the column using a linear gradient from 10 to 200 mM potassium phosphate, pH 7.2, containing 1 mM EDTA (PBE, pH 7.2). The fractions containing AdoHcy hydrolase, as monitored by activity and SDS−PAGE, were combined and concentrated to approximately 2 mg/mL and stored at 4 °C in 10 mM PBE, pH 7.2. The concentration of protein was determined by the method of Bradford (*14*). Bovine serum albumin was used as a standard. The purity of the enzyme was determined by SDS−PAGE (12% gel) stained with Coomassie Brilliant Blue R-250.

Preparation of the Apo Form and Reconstituted NAD$^+$ Form of AdoHcy Hydrolases. Preparation of the apo forms of wild-type and mutant AdoHcy hydrolases and reconstitution to full occupancy by NAD^+ (4 equiv per tetramer) were carried out according to the protocol described previously (*13*). Briefly, the enzyme was precipitated by adding saturated ammonium sulfate buffer, pH 2.9, up to 70% saturation, and incubated on ice for 15 min. The sample was centrifuged for 15 min in a Beckman J2-21 centrifuge using a JA-14 rotor at 10000 rpm. The supernatant was discarded, and the pellet was dissolved in 25 mM phosphate buffer, pH 7.2, containing 1 mM EDTA. The process was repeated with saturated ammonium sulfate, pH 2.9. The solution was monitored by fluorescence spectrometry to ensure that no cofactor remained bound. The enzyme was then precipitated with saturated ammonium sulfate buffer, pH 7.2, up to 70% saturation on ice. After centrifugation the supernatant was discarded. The pellet was dissolved in 50 mM phosphate buffer, pH 7.2, containing 1 mM EDTA. All solutions used in these steps were supplemented with 1 μM DTT.

Reconstitution of the apoenzyme to full NAD^+ occupancy was accomplished by incubation with 2 mM NAD^+ at 4 °C overnight. The enzyme was then passed through a G-25 Sephadex size-exclusion column to remove excess unbound cofactor. The enzyme was eluted from the column with 50 mM phosphate buffer, pH 7.2, containing 1 mM EDTA, and stored at 4 °C.

Determination of the Structural Characteristics of Mutants of AdoHcy Hydrolase. Circular dichroism (CD) spectra of AdoHcy hydrolase were measured using a Jasco J-710 spectropolarimeter (Jasco Corp., Tokyo, Japan) and a temperature-jacketed spectral cell (path length: 1 cm). Spectra were recorded at 1 nm intervals from 200 to 240 nm at 37 °C for 0.05 mg/mL enzyme (wild type and mutant) in 25 mM Tris buffer, pH 7.2. The apparent α-helix content was determined by the method of ridge regression (*15*), using the computer program Contin (*16*).

Gel permeation chromatography was performed using an FPLC system (Pharmacia LKB) equipped with a Superdex 200 HR 10/30 size-exclusion column. The column was equilibrated with 25 mM Tris buffer, pH 7.2. The proteins were monitored at 280 nm, and the peak areas were integrated automatically by the FPLC system controller (Controller LCC-500 PLUS, Pharmacia LKB).

Determination of Specific Activities of the Mutants of AdoHcy Hydrolase: AdoHcy Hydrolysis. AdoHcy hydrolase activity in the hydrolytic direction was measured by a modified version of the procedure described previously (*13*). The reaction mixture contained 10 μL of 1 mg/mL Ado deaminase, a measured amount of wild-type or mutant enzyme, and various amounts of AdoHcy. Each mixture was brought to 490 μL with 50 mM potassium phosphate, pH 7.2, containing 1 mM EDTA (PBE buffer). The reaction was run for 5 min at 37 °C and terminated by the addition of 10 μL of 5 N $HClO_4$. After centrifugation, concentrations of inosine (product of the adenosine deaminase coupling reaction) were determined by reversed-phase HPLC using a C18 column (Vydac C18, 5 μm, 250 × 4.5 mm, Hesperia, CA) with a flow rate of 1 mL/min of 25 mM phosphate buffer, pH 3.2, containing 10 mM heptanesulfonic acid with a linear gradient of 2−98% acetonitrile over 25 min. Products were monitored spectrophotometrically at 250 nm. The concentration of inosine was determined by comparison of the peak area with a standard curve made using known quantities of inosine. Activity in international units (micromoles per milligram per minute) was calculated from the inosine concentration, amount of enzyme, and the duration of reactions.

Determination of Specific Activities of the Mutants of AdoHcy Hydrolase: AdoHcy Synthesis. AdoHcy hydrolase activity in the synthetic direction was measured using the method described by Yuan et al. (*13*). The reaction mixture (total volume of 500 μL) contained a saturating amount of Hcy, various amounts of Ado, and an amount of enzyme determined by the activity of each mutant. Reactions were carried out in 50 mM potassium phosphate buffer, pH 7.2, containing 1 mM EDTA. The reaction was run for 5 min at 37 °C and terminated by the addition of 10 μL of 5 N $HClO_4$. After centrifugation, AdoHcy concentrations were determined by reversed-phase HPLC using a C18 column (Vydac C18, 5 μm, 250 × 4.5 mm) with a flow rate of 1 mL/min of 25 mM phosphate buffer, pH 3.2, containing 10 mM heptanesulfonic acid with a linear gradient of 2−98% acetonitrile over 25 min. AdoHcy was monitored at 258 nm. The concentration of AdoHcy was determined by comparison of the peak area with a standard curve made using known quantities of AdoHcy. Activity in international units (micromoles per milligram per minute) was calculated from the AdoHcy concentration, amount of enzyme, and the duration of reactions.

Determination of Specific Activities of the Mutants of AdoHcy Hydrolase: AdoHcy Hydrolysis and 3′-Oxidative Activity. The oxidation of a mechanism-based inhibitor, NepA, by AdoHcy hydrolases was assayed by measuring the rate of formation of NADH. The enzyme at 10 μM reacted with 200 μM NepA in the chamber of a stopped-

Table 1: Rate Constants for Catalysis and Model Reactions of AdoHcy Hydrolase[a]

mutation	k_{cat} ($1.2\ s^{-1}$)[b]	k_{cat}/K_M ($1.5 \times 10^5\ M^{-1}\ s^{-1}$)[b]	redox model reaction ($182\ s^{-1}$)[b]	el/ad model reaction ($0.013\ s^{-1}$)[b]
E156A	$2.6(0.1) \times 10^{-2}$	$3.6(1.2) \times 10^{-3}$	0.17(0.2)	$1.84(0.2) \times 10^{-4}$
N181A	$2.6(0.1) \times 10^{-2}$	$6.6(2.2) \times 10^{-4}$	$7.33(0.7) \times 10^{-2}$	$5.48(0.6) \times 10^{-5}$
K186A	$3.5(0.6) \times 10^{-4}$	$6.3(2.1) \times 10^{-6}$	$6.54(0.7) \times 10^{-4}$	$1.78(0.2) \times 10^{-6}$
D190A	$4.0(0.3) \times 10^{-2}$	$6.8(2.3) \times 10^{-4}$	0.143(0.2)	$3.8(0.4) \times 10^{-4}$
N191A	$9.6(0.4) \times 10^{-3}$	$6.4(2.1) \times 10^{-4}$	0.25(0.03)	$3.85(0.4) \times 10^{-5}$

[a] Parenthetical values are estimated standard deviations. [b] Values of the rate constants for the wild-type enzyme.

flow instrument (Hi-Tech Scientific SF-41 Canterbury) at 37 °C. NADH content was monitored at 330 nm. All reactions were carried out in 50 mM potassium phosphate buffer, pH 7.2, containing 1 mM EDTA. Obtained data were plotted and analyzed using Microcal Origin 6.0 software.

Determination of Specific Activities of the Mutants of AdoHcy Hydrolase: 5′-Addition Activity. The activity toward EDDFHA by AdoHcy hydrolases was assayed by measuring the rate of 6′-deoxy-6′-fluoro-5′-hydroxyhomoadenosine (DFHHA) formation. The mutant enzymes, at appropriate concentrations, were incubated with 200 μM EDDFHA in 500 μL of 50 mM PBE buffer, pH 7.2, at 37 °C for 30 min. The reaction was terminated by addition of 10 μL of 5 N $HClO_4$. After centrifugation, the supernatants were analyzed by HPLC on a C18 reversed-phase column (Vydac C18, 5 μm, 250 × 4.5 mm). The column was operated at a flow rate of 1 mL/min solvent with a linear gradient of 2−98% solvent over 25 min. Solvent A was 25 mM phosphate, pH 3.2, and 10 mM heptanesulfonic acid. Solvent B was 80% acetonitrile and 20% 2-propanol. One of the products, DFHHA, was monitored at 258 nm. Characterization of the products generated by the incubation of EDDFHA with AdoHcy hydrolase was described previously (*11*).

Determination of NAD^+ and NADH Content of Mutant AdoHcy Hydrolases as Isolated. NAD^+ was released by the addition of 10 μL of 5 N $HClO_4$. The concentration of NAD^+ was analyzed by HPLC as described above. NAD^+ was monitored at 258 nm. NADH content was directly determined by measuring the absorbance at 340 nm and comparing to the standard curve.

RESULTS

Mutants of Human AdoHcy Hydrolase Retain the Structure of the Wild-Type Enzyme. Point mutations of human AdoHcy hydrolase were successfully created by site-directed mutagenesis. Residues E156, N181, K186, D190, and N191 were individually mutated to alanine (A). SDS−PAGE gels (data not shown) indicated that the mutants were fully expressed intact proteins with the correct monomer molecular weight. Native PAGE gels (data not shown) demonstrated that each of the mutant enzymes, like the wild type, contained four of the monomeric subunits. The tetrameric quaternary structure of AdoHcy hydrolase was thus maintained in the five mutants. Analysis of CD data (not shown) for the wild-type and mutant forms of AdoHcy hydrolase suggests that fractions of α-helical and β-sheet structures have not significantly shifted in the mutants, indicating a maintenance of the secondary structure.

Effects of Mutations on Isolated Cofactor Content. The cofactor contents of the wild-type AdoHcy hydrolase, as isolated from the expression and purification processes, were consistent with reported values (*17*); all of the mutants had very similar cofactor binding levels, although the values obtained reflect characteristics of the particular isolation procedure and need not to be reproducible. To ensure that small differences in cofactor occupancy did not contribute to differences in apparent catalytic activity, mutant enzymes were prepared in reconstituted form with full NAD^+ occupancy.

Mutations of AdoHcy Hydrolase Have Significant Effects on Catalytic Activities. Catalytic rate constants for overall catalysis in the hydrolytic direction, for the 3′-oxidative activity as measured by the NepA model reaction, and for the 5′-addition activity as measured by the EDDFHA reaction are shown in Table 1. All five mutants caused dramatic decreases in the hydrolytic activity of AdoHcy hydrolase. Among them, the K186A mutant caused the highest increase in Gibbs free energy change ($\Delta\Delta G$ value), while the E156A mutant showed the lowest increase in the same value. Mutants N181A, D190A, and N191A exhibited comparable drastic changes in free energy value, but they are lower than that of K186A mutant, although much higher than mutant E156A. All mutations led to reduced rates in both model catalytic reactions, the minimum rate reduction factor being around 30 and the maximum about 280000.

DISCUSSION

The Mutations Do Not Change the Structural Integrity of AdoHcy Hydrolase. The five mutations carried out here appear not to exert significant effects on the secondary structure, as reflected in CD experiments, or the quaternary (homotetrameric) structure, as reflected by the gel-filtration experiments and FPLC analysis. This indicates that interpretations of the kinetic effects of these mutations can be based on the assumption that the available crystallographic structures of AdoHcy hydrolase provide reasonable guides to the three-dimensional positions of enzyme ligands such as substrate and cofactor in relationship to the alanine side chain that now replaces the mutated side chains.

Mutations of the Chosen Residues Reduce the Rate Constants for the Redox Model Reaction by ∼2−5 Orders of Magnitude. The assignment of potential catalytic roles shown in Figure 4 suggested that K186 should play a major catalytic role, being directly involved in acid−base or hydrogen-bonding acceleration of both the redox and elimination/addition partial reactions. The other residues were suggested to take more minor roles: in appropriate localization of the K186 side chain (N181, N191), in orientation of the substrate for effective transition-state stabilization (D190), and in "proton management", or maintenance of the appropriate protonation state of K186 for its catalytic tasks (E156).

Table 2: Factors by Which Rate Constants for Catalysis and Model Reactions of AdoHcy Hydrolase Are Reduced by Mutations and Corresponding Increases in Free Energy of Activation[a]

mutation	k_{cat} ($1.2\ s^{-1}$)[b]	k_{cat}/K_M ($1.5 \times 10^5\ M^{-1}\ s^{-1}$)[b]	redox model reaction ($182\ s^{-1}$)[b]	el/ad model reaction ($0.013\ s^{-1}$)[b]
E156A	46	42	1071	71
	(10)	(9)	(17)	(11)
N181A	46	227	2483	237
	(10)	(13)	(19)	(14)
K186A	3429	23800	278300	7303
	(20)	(25)	(31)	(22)
D190A	30	221	1273	34
	(8)	(13)	(18)	(9)
N191A	125	234	728	338
	(12)	(14)	(16)	(14)

[a] The corresponding increases in free energy of activation are given in parentheses below each factor (in kJ/mol). Rate reduction factors are reliable to about ±30%. The changes in free energy of activation are reliable to around ±2 kJ/mol. [b] Values of the rate constants for the wild-type enzyme.

These expectations are confirmed in the results for the redox model reaction (Table 2). The largest rate reduction factor of 280000 ($\Delta\Delta G^* = +31$ kJ/mol) is for the K186A mutation and presumably reflects the loss of all or, more likely, a part of the acid−base catalytic function of this residue in the hydride transfer from C3′ of NepA to NAD^+. Possibly, the fact that the rate reduction is not still more severe suggests that catalysis by K186 can be assumed (at least in this model reaction) by some other functional groups in the active site. The concept of ancillary roles for N181 and N191, in maintaining the K186 side chain in a correct location for effective catalysis, is consistent with reductions in the redox rate constant by factors of 2500 and 700 ($\Delta\Delta G^* = +16-19$ kJ/mol) upon mutation of these residues to alanine. If this interpretation of their catalytic roles is correct, it suggests that, in any acid−base or hydrogen-bonding catalytic function, a lysine side chain may require buttressing interactions to achieve the needed localization of its flexible side chain and that, without such buttressing, the catalytic effectiveness may be reduced by around 3 orders of magnitude. The putative substrate orientation function of D190 to favor transition-state stabilization by other residues is again consistent with a mutational rate constant reduction factor of 1300 ($\Delta\Delta G^* = +18$ kJ/mol), although nearly any magnitude would also be consistent with such a role, the quantitative value of which has not been assessed in general. Finally, a similar factor of 1100 ($\Delta\Delta G^* = +17$ kJ/mol) for the E156A mutation is readily reconciled with its suggested proton management function but constitutes no real test of the hypothesis because no basis for estimating the expected quantitative significance of such a function is provided by the data currently available.

These results should also be seen in the light of imperfections in the model reaction. The caption of Figure 5 notes both similarities and differences between the actual partial reaction and the model reaction.

Mutations of the Chosen Residues Reduce the Rate Constants for the Elimination/Addition Model Reaction by ∼1−4 Orders of Magnitude. The mutations also universally reduce the rate constants for the elimination/addition model reaction, in roughly the same order for the different residues as in the redox model reaction, but with the magnitudes of the rate reductions reduced by about 1 order of magnitude. This set of smaller effects could indicate a smaller importance of the mutated residues in acceleration of the elimination/addition partial reaction than in acceleration of the redox reaction; however, it may instead arise from the poorer correspondence of the elimination/addition model reaction to the partial reaction in the actual catalytic cycle than is true for the redox model reaction (see Figures 5 and 6). In particular, in the actual elimination/addition partial reaction of the catalytic cycle, elimination and addition occur across the 4′−5′ linkage, proton removal/donation occurs at C4′, and the C-3′ position is at the keto stage of oxidation. In the model reaction, elimination and addition occur across the 5′−6′ linkage (*11*), proton removal/donation does not occur at C4′, and the C-3′ position is at the hydroxyl stage of oxidation.

Nevertheless, the relative magnitudes of the mutational rate reductions may give some idea of the roles of these five residues in the elimination/addition partial reaction. The largest effect of about 7000-fold ($\Delta\Delta G^* = +22$ kJ/mol) is again for the K186A mutation, tending to confirm a primary catalytic role for this residue. In the catalytic cycle, this may be stabilization of negative charge on the C-3′ carbonyl oxygen in the transition states of 4′−5′ elimination and addition reactions. In the model reaction, a related hydrogen-bonding interaction with the C-3′ hydroxyl may serve to orient the substrate molecule for effective addition across the 5′−6′ linkage. Smaller effects of ∼200−300-fold ($\Delta\Delta G^* = +14$ kJ/mol) for N181 and N191 are also consistent with their role in localizing the ϵ-amino group of K186 for its interaction at the 3′-center. The small effects for D190 and E156 (30−70-fold, $\Delta\Delta G^* = +9-11$ kJ/mol) are again consistent with roles in orientation and proton management, the small size suggesting that either the partial reaction is reasonably insensitive to these roles or that other residues or water molecules can assume the roles when the wild-type side chains are removed.

Here, too, the results should also be seen in the light of imperfections in the model reaction. The caption of Figure 6 notes both similarities and differences (which are particularly great in the EDDFHA case) between the actual partial reaction and the model reaction.

The Energetic Mutational Effects on the Catalytic Parameters Should Be Linear Combinations of the Effects on the Partial Reactions. Figure 7 shows a minor algebraic exercise that generates the hypothesis that the mutation induced increases in kinetic barrier height $\Delta\Delta G^*$ for k_{cat} and for k_{cat}/K_M for the hydrolytic direction of the catalytic cycle should be simple linear combinations of the $\Delta\Delta G^*$ values for the partial reactions. The coefficients of the linear combination would then be the fractional degree to which each of the partial reactions determines the rate for each of the catalytic parameters. If the mutational data for the model partial reactions, shown in Table 2, are accepted as adequate representations of the effects on the actual partial reactions, then the final equation of Figure 7 becomes a direct prediction with no adjustable parameters. The results of the predictions can then be compared with the data for k_{cat} and k_{cat}/K_M, also taken from Table 2.

The Model of Figure 7 Describes the Observations for k_{cat}/K_M but Requires an Adjustment of 5 kJ/mol for k_{cat}. Figure 8 shows the predictions of the mutational effects on k_{cat}/K_M

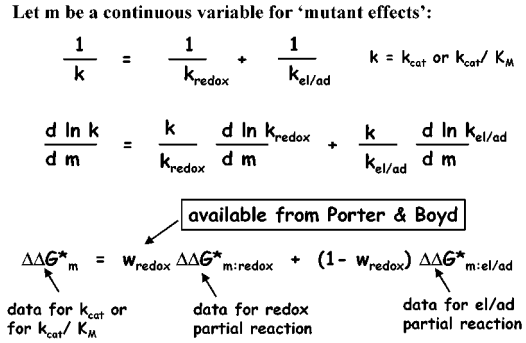

FIGURE 7: Development of the expected relationship between mutation-induced increases in free energy of activation $\Delta\Delta G^*$ for k_{cat} and for k_{cat}/K_M and the corresponding increases for the redox partial reaction $\Delta\Delta G^*_{redox}$ and for the elimination/addition partial reaction $\Delta\Delta G^*_{el/ad}$. At the top, the rate constants k_{cat} and k_{cat}/K_M are expressed as steady-state combinations of the partial reaction rate constants (which will, of course, be different for k_{cat} and for k_{cat}/K_M). In the second equation, the rate constants k_{cat} and k_{cat}/K_M are taken to be a function of the hypothetical variable *m*, which describes the effects of mutation. The equation results from calculating d*k*/d*m* and shows the mutational effects on the free energy barrier (proportional to ln *k*) for the overall rate constants to be linear combinations of the effects on the free energy barriers for the partial reactions. The coefficients of the linear equation are the fractional degrees to which the particular partial reaction limits the rate for each of the rate constants, and the coefficients therefore sum to unity. From the detailed studies of Porter and Boyd (*18*, *19*) and Porter (*20*), we have available the values of each of the four coefficients. The final equation converts the various d(ln *k*)/d*m* to $\Delta\Delta G^*$. If the mutational data of Table 2 for effects on the model partial reactions are taken to be adequate representations of the effects on the actual partial reactions, then there are no adjustable variables and the equations are direct predictions of the mutational effects on $\Delta\Delta G^*$ for k_{cat} and k_{cat}/K_M.

and on k_{cat}, made according to the final equation in Figure 7 and compared with the observations from Table 2. We calculate from the rate constants of Porter and Boyd (*18*, *19*) and Porter (*20*) the information that the redox partial reaction is 12% rate-limiting for k_{cat}/K_M [i.e., $(k_{cat}/K_M)/(k_{cat}/K_M)_{redox} = 0.12$] and that the elimination/addition partial reaction is therefore 88% rate-limiting for k_{cat}/K_M; similarly for k_{cat}, the redox partial reaction is 45% rate-limiting and the elimination/addition is 55% rate-limiting. We take the model reaction data of Table 2 correctly to represent the effects on the actual model reactions.

As Figure 8 shows, the predictions for k_{cat}/K_M were in agreement with the observations. This kinetic parameter is the net rate constant for conversion of free enzyme (open structure) and free AdoHcy to a series of transition states up through that for the first irreversible catalytic step, which is either release of Hcy or a preceding step. If we neglect the effect of mutations on the free enzyme, the effects represented in the mutational effect on k_{cat}/K_M will be transition-state effects. The agreement with observations of the predictions made on the basis of model reaction data thus suggests that the model reactions are reasonably representative of the mutational effects in the transition states of both partial reactions.

The rate constant k_{cat} brings into the picture the role of enzyme−substrate, enzyme−intermediate, and enzyme−product interactions because this constant describes the conversion of these states each to a set of transition states that follow it on the reaction path. All or most of the reactant-state and transition-state complexes are formed with the

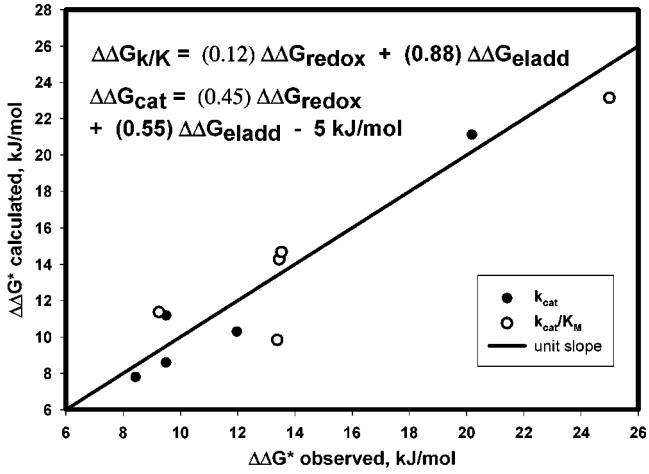

FIGURE 8: Mutational effects on the rate constants for AdoHcy hydrolase-catalyzed hydrolysis of AdoHcy, as calculated (ordinate) from the final equation of Figure 7 with the coefficients shown computed from the rate constants of Porter and Boyd (*18*, *19*) and Porter (*20*). Mutational effects on the two partial reactions were taken as the effects in model partial reactions, given in Table 2. The observed mutational effects on the catalytic parameters (abscissa) were taken from Table 2. The solid line is the line of unit slope, reflecting agreement of prediction and observation. The predictions for k_{cat}/K_M (open circles) scatter about the line of agreement with observations. The predictions for k_{cat} formed a line of unit slope, but it lay about 5 kJ/mol positive of the line of agreement, showing that the prediction indicated that the mutant enzymes should uniformly react somewhat less than 10-fold more slowly than in fact they did. Subtraction of 5 kJ/mol from the predictions produced agreement with the observations.

enzyme in its closed state. Figure 8 shows that a simple application of the relationship derived in Figure 7 leads to correct relative values of $\Delta\Delta G^*$, but all of these are approximately 5 kJ/mol too large to lie on the line of agreement between prediction and observation in Figure 8. Thus, the points plotted in Figure 8, which scatter around the line of agreement, are the predicted values less 5 kJ/mol. The prediction therefore suggests that the mutant enzymes should all react nearly 10-fold more slowly than they actually do.

If one concludes from the success of the k_{cat}/K_M prediction, where only enzyme−transition state interactions were an issue, that the model partial reactions are accurately measuring the mutational effects on enzyme−transition state interactions, then the failure of the k_{cat} prediction by a uniform 5 kJ/mol increment may be ascribed to the fact that reactant-state interactions of enzyme with substrate, intermediates, and product have been brought in by the k_{cat} data. These interactions may not be well measured by the model reactions, and therefore, the required subtraction of 5 kJ/mol from the k_{cat} data may correct for this deficiency in the model reactions. If that is correct, then the wild-type enzyme is stabilizing its reactant-state catalytic cycle ligands by an average of 5 kJ/mol by interactions that are not reproduced by the model reactions and that are abolished by the mutations. These particular forms of reactant-state stabilization will increase the average barrier height by around 5 kJ/mol and thus slow passage through the catalytic cycle by about 7−8-fold. This small sacrifice in catalytic power could be necessary to achieve other catalytic aims, such as sequestering the labile intermediate compounds from abortive loss to the solvent.

CONCLUSIONS

Residue K186 appears to be implicated as a primary catalytic residue in both partial reactions. A logical assignment would be that K186 serves as an acid−base catalyst (a) to stabilize 3′ redox transition states by proton donor/acceptor interaction at the 3′-keto/hydroxyl during the redox partial reaction and (b) to stabilize negative charge on the 3′-keto oxygen center in the transition states for elimination and addition across the 4′−5′ linkage in the elimination/addition partial reaction. A secondary role of guiding the flexible K186 side chain into the right location for its primary functions is consistent with the smaller mutational effects for N181 and N191. Secondary roles are also reasonable for D190 (orientation of the ribose structure of the substrate for optimal transition-state stabilization in both partial reactions) and E156 (proton management, or assisting in maintenance of the proper protonation state of K186 throughout the catalytic cycle). A larger set of mutations and broader characterization of each would be required to establish more definitely these catalytic hypotheses.

It may not be coincidental that all of these residues are located in the hinge region of the enzyme that links the two domains that move in the open form of the enzyme and become closed against each other during the catalytic cycle. It is entirely possible that their chemical reactions involving these residues, particularly in the redox partial reaction, may be linked to the cessation and onset of domain/domain motion at the beginning and end, respectively, of the catalytic cycle. Work is currently underway to explore such a hypothesis.

REFERENCES

1. Palmer, J. L., and Abeles, R. H. (1979) *J. Biol. Chem. 254*, 1217−1226.
2. Turner, M. A., Yang, X., Yin, D., Kuczera, K., Borchardt, R. T., and Howell, P. L. (2000) *Cell Biochem. Biophys. 33*, 101−125.
3. Guillerm, G., Guillerm, D., Vandenplas-Witkowki, C., Rogniaux, H., Carte, N., Leize, E., Van Dorsselaer, A., De Clercq, E., and Lambert, C. (2001) *J. Med. Chem. 44*, 2743−2752.
4. Robins, M. J., Wnuk, S. F., Yang, X., Yuan, C. S., Borchardt, R. T., Balzarini, J., and De Clercq, E. (1998) *J. Med. Chem. 41*, 3857−3864.
5. Chiang, P. K. (1998) *Pharmacol. Ther. 77*, 115−134.
6. Nygard, O., Vollset, S. E., Refsum, H., Brattstrom, L., and Ueland, P. M. (1999) *J. Intern. Med. 246*, 425−454.
7. Hu, Y., Komoto, J., Huang, Y., Gomi, T., Ogawa, H., Takata, Y., Fujioka, M., and Takusagawa, F. (1999) *Biochemistry 38*, 8323−8333.
8. Huang, Y., Komoto, J., Takata, Y., Powell, D. R., Gomi, T., Ogawa, H., Fujioka, M., and Takusagawa, F. (2002) *J. Biol. Chem. 277*, 7477−7482.
9. Turner, M. A., Yuan, C. S., Borchardt, R. T., Hershfield, M. S., Smith, G. D., and Howell, P. L. (1998) *Nat. Struct. Biol. 5*, 369−376.
10. Matuszewska, B., and Borchardt, R. T. (1987) *J. Biol. Chem. 262*, 265−268.
11. Yuan, C. S., Wnuk, S. F., Liu, S., Robins, M. J., and Borchardt R. T. (1994) *Biochemistry 33*, 12305−12311.
12. Coulter-Karis, D. E., and Hershfield, M. S. (1989) *Ann. Hum. Genet. 53*, 169−175.
13. Yuan, C. S., Yeh, J., Squier, T. C., Rawitch, A., and Borchardt, R., T. (1993) *Biochemistry 32*, 10414−10422.
14. Bradford, M. M. (1976) *Anal. Biochem. 72*, 248−254.
15. Provencher, S. W., and Glockner, J. (1981) *Biochemistry 20*, 33−37.
16. Venyaminov, S. Y., and Yang, J. T. (1996) in *Circular Dichroism and the Conformational Analysis of Biomolecules* (Fasman, G. D., Ed.) pp 69−107, Plenum Press, New York.
17. Hershfield, M. S., Aiyar, V. N., Premakumar, R., and Small, W. C. (1985) *Biochem. J. 230*, 43−52.
18. Porter, D. J. T., and Boyd, F. L. (1991) *J. Biol. Chem. 266*, 21616−21625.
19. Porter, D. J. T., and Boyd, F. L. (1992) *J. Biol. Chem. 267*, 3205−3213.
20. Porter, D. J. T. (1993) *J. Biol. Chem. 268*, 63−73.
21. Yin, D., Yang, X., Hu, Y., Kuczera, K., Schowen, R. L., Borchardt, R. T., and Squier, T. C. (2000) *Biochemistry 39*, 9811−9818.

BI025771P